EurJIC European Journal of Inorganic Chemistry

ChemPubSoc Europe

FULL PAPER

DOI:10.1002/ejic.201201089

Four Members of the Sandwich-Type Polytungstophosphate Family Based on Pentalacunary $[HPW_7O_{28}]^{8-}$ Building Blocks

CLUSTER ISSUE

Dongdi Zhang,[a,b] Yanhui Zhang,[a,b] Juan Zhao,[a,b] Pengtao Ma,[a,b] Jingping Wang,*[a,b] and Jingyang Niu*[a,b]

Dedicated to Professor Michael T. Pope on the occasion of his 80th birthday

Keywords: Cluster compounds / Polyoxometalates / Sandwich complexes / Tungsten / Electrocatalysis

Four dimeric mononuclear sandwich-type tungstophosphate clusters of $Na_{12}H[Fe^{III}(HPW_7O_{28})_2]\cdot 44H_2O$ (**1**) and $Na_{14}[M(HPW_7O_{28})_2]\cdot 44H_2O$ {M = Co^{II} (**2**), Cd^{II} (**3**), Mn^{II} (**4**)} were successfully synthesized by reaction of $Na_2WO_4\cdot 2H_2O$, H_3PO_4, and CH_3COOH with $FeCl_3\cdot 6H_2O$, $Co(CH_3COO)_2\cdot 4H_2O$, $CdSO_4\cdot 8H_2O$, and $Mn(CH_3COO)_2\cdot 4H_2O$, respectively. Single-crystal X-ray diffraction analysis revealed that **1**–**4** are essentially isomorphous and crystallize in the triclinic space group $P\bar{1}$. Complexes **1**–**4** consist of two $[HPW_7O_{28}]^{8-}$ units incorporating a single Fe^{III}, Co^{II}, Cd^{II}, and Mn^{II} ion, respectively. Furthermore, the electrocatalytic behaviors of **1**–**4** in the reduction of nitrite were investigated.

Introduction

Polyoxometalates (POMs) are metal oxide cluster compounds that are mainly composed of high-valent early transition metals (usually Mo, W, V, Nb, and Ta).[1] Their intriguing structural diversity[2] and remarkable chemical properties[3] allow them to have many potential applications in diverse fields including catalysis, materials science, medicine, and nanotechnology.[4] Lacunary (or vacant) POMs, obtained by removing one or more octahedral metal atoms from the plenary POMs, have received special attention in POM chemistry.[1b,2d,4d]

It is well known that vacant POM precursors, for example, $[\alpha\text{-}PW_{11}O_{39}]^{7-}$, $[\alpha\text{-}XW_{11}O_{39}]^{8-}$ (X = Si, Ge), $[\alpha\text{-}P_2W_{17}O_{61}]^{10-}$, $[\gamma\text{-}PW_{10}O_{36}]^{7-}$, $[\gamma\text{-}XW_{10}O_{36}]^{8-}$ (X = Si, Ge), $[\alpha\text{-}PW_9O_{34}]^{9-}$, $[\alpha\text{-}XW_9O_{34}]^{10-}$ (X = Si, Ge), $[\alpha\text{-}P_2W_{15}O_{56}]^{12-}$, $[\alpha\text{-}H_2P_2W_{12}O_{48}]^{12-}$, and $[\alpha\text{-}H_7P_8W_{48}O_{184}]^{33-}$, can be easily synthesized by one- or two-step processes in high yield.[5] These lacunary units can act as excellent inorganic multidentate ligands and can be functionalized by either grafting or incorporating lanthanides, organometallic entities, or transition metals in many different ways to afford a large number of substituted and functionalized POMs.[6] In particular, considerable attention has been directed towards the exploration of transition-metal (TM)-substituted heteropolytungstates (HPTs) by reaction of TMs with lacunary POMs, especially those derived from the "parent" Keggin-type HPTs, as follows, monovacant ($XW_{11}O_{39}^{n-}$: X = P, Si, Ge, Zn, Fe),[7] divacant ($XW_{10}O_{36}^{n-}$: X = P, Si, Ge),[8] trivacant ($XW_9O_{34}^{n-}$: X = Si, Ge, Se, Te, P, As, Sb, Bi, Ni, Co, Zn, Fe, etc.),[9] tetravacant ($XW_8O_{31}^{n-}$: X = Si, Ge).[10]

Interestingly, relative to the abundant amount of research on TM-HPTs, the number of structurally characterized TM-containing pentavacant Keggin polyoxomolybdates[11] and polyoxotungstates[12] is still rather limited. Hitherto, to the best of our knowledge, only four types of heptatungstate $\{XW_7\}$ (X = P,[12a,12b] As,[12a] V,[12c] Te[12d]) polyanions are known. In 2005, Kortz and co-workers prepared the pioneering examples of ruthenium(II)-supported heteropolyanions $[HXW_7O_{28}Ru(dmso)_3]^{6-}$ (X = P, As), which are composed of a $Ru(dmso)_3$ group attached to an unprecedented heptatungstate fragment.[12a] Subsequently, Wu et al. communicated the heptatungstovanadate analogue $[HVW_7O_{28}Ru(dmso)_3]^{6-}$ in 2010.[12c] The same year, the Boskovic group reported unfunctionalized POMs based on the Te-containing lacunary Keggin ions $[Te_2W_{16}O_{58}(OH)_2]^{14-}$ and $[Te_2W_{18}O_{62}(OH)_2]^{10-}$.[12d] These two polyoxoanions contain a previously unreported lacunary Keggin building block $[A\text{-}\alpha\text{-}TeW_7O_{28}]^{10-}$. These findings indicate that it is difficult to obtain $\{XW_7\}$-based compounds,

[a] Polyoxometalates Chemistry Key Laboratory of Henan Province, College of Chemistry and Chemical Engineering, Henan University,
Kaifeng, Henan 475004, China
Fax: +86-378-3886876
E-mail: jyniu@henu.edu.cn
Homepage: http://ccce.henu.edu.cn
[b] Institute of Molecular and Crystal Engineering, College of Chemistry and Chemical Engineering, Henan University,
Kaifeng, Henan 475004, China
E-mail: jpwang@henu.edu.cn

Supporting information for this article is available on the WWW under http://dx.doi.org/10.1002/ejic.201201089.

but it is nevertheless interesting. Therefore, it is an ongoing challenge to design and synthesize novel high-lacunary Keggin-type POMs. In general, one effective approach is to use high-lacunary fragments as precursors to react with TM centers to make TM-substituted or -incorporated HPTs by conventional aqueous solution methods. However, it should be noted that formation of POMs occurs through self-assembly, which depends more on the reaction conditions (e.g., pH value, concentration and ratio of reagents, ionic strengths) than on the type of polyanion precursors used.[13]

Herein we present four new TM-incorporated heptatungstophosphates (HTPs) $Na_{12}H[Fe^{III}(HPW_7O_{28})_2]\cdot 44H_2O$ (**1**) and $Na_{14}[M(HPW_7O_{28})_2]\cdot 44H_2O$ {M = Co^{II} (**2**), Cd^{II} (**3**), Mn^{II} (**4**)} by reaction of Na_2WO_4, H_3PO_4, and CH_3COOH with $FeCl_3\cdot 6H_2O$, $Co(CH_3COO)_2\cdot 4H_2O$, $CdSO_4\cdot 8H_2O$, and $Mn(CH_3COO)_2\cdot 4H_2O$, respectively. We also investigated the electrochemical properties of **1**–**4**, and the results demonstrate that compound **1** exhibit moderately good electrocatalytic activity towards the reduction of nitrite.

Results and Discussion

Synthesis

As mentioned in the introduction, TM-containing high-lacunary POMs remain largely unexplored. Therefore, the synthesis of $\{XW_7\}$-based TM-incorporated architectures has become an attractive but challenging goal. In this paper, HPW_7O_{28}-based mononuclear sandwich-type HTPs **1**–**4** were successfully synthesized by conventional beaker methods (Scheme 1).

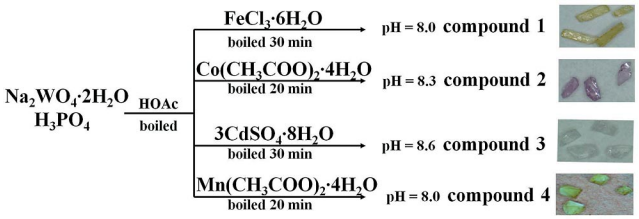

Scheme 1. Illustration of the synthesis routes of **1**–**4**.

In general, the synthesis of **1**–**4** consists of two steps. A solution of $Na_2WO_4\cdot 2H_2O$, H_3PO_4, and acetic acid was first boiled, and then heated at reflux for 30 (for **1**) or 20 (for **2**–**4**) min after the addition of the corresponding TM. These two steps appear to be crucial for the preparation of **1**–**4**. (1) If the reaction is performed in the absence of acetic acid, **1**–**4** are not formed. (2) The pH should be carefully adjusted to 6.5–8.0 for **1** and **4** and to 6.5–9.0 for **2** and **3**. When the pH is lower than 6.5, the title compounds cannot be isolated; conversely, when the pH is higher than the upper limit value, only an abundance of unknown amorphous powders was obtained. Additionally, the optimum pH value for **1**–**4** is 8.0, 8.3, 8.6 and 8.0, respectively. (3) The temperature of step 1 plays an important role in facilitating the reaction, as the yield improves greatly with boiling. (4) We also made great efforts to prepare other TM analogues. Unfortunately, the crystals of the Cr^{III} and Ni^{II} compounds effloresced as soon as they were transferred out of the mother solution so that we could not obtain satisfying crystal data. However, the IR spectra of these two compounds are very similar to those of **1**–**4** (Figures S1 and S2, Supporting Information), which suggests that they might be $[Cr(HPW_7O_{28})_2]^{13-}$ and $[Ni(HPW_7O_{28})_2]^{14-}$, respectively. Moreover, we have not isolated the Cu^{II} and Zn^{II} analogues to date. (5) As is known, the stoichiometry of the synthetic reaction generally has a decisive influence on the structure of the product in POM chemistry. The results show that the optimal ratio of TM/WO_4^{2-} is 1:14, 1:29, 1:14, and 1:15 for **1**, **2**, **3**, and **4**, respectively. Obviously, the ratio of TM/WO_4^{2-} is equivalent to its stoichiometric ratio, except for the case of **2**. Only when the ratio is increased to 1:29 could we obtain crystals of **2** suitable for X-ray crystallography, but these crystals were accompanied by other purple crystals of $[Co_7(H_2O)_2(OH)_2P_2W_{25}O_{94}]^{16-}$.[14]

In addition, we also tried to synthesize **1**–**4** by increasing the volume of water from 10 to 30 mL but without success, and this implies that the initial concentration of sodium tungstate may be one of the phase-determining factors in these syntheses, which agrees well with the findings of Yan et al.[6d]

Structural Description

Single-crystal X-ray diffraction analysis revealed that $[Fe^{III}(HPW_7O_{28})_2]^{13-}$ (**1a**), $[Co^{II}(HPW_7O_{28})_2]^{14-}$ (**2a**), $[Cd^{II}(HPW_7O_{28})_2]^{14-}$ (**3a**), and $[Mn^{II}(HPW_7O_{28})_2]^{14-}$ (**4a**) are isostructural and crystallize in the triclinic space group $P\bar{1}$. Therefore, only the structure of **1a** is discussed here.

Polyanion **1a** is composed of two pentalacunary Keggin $\{HPW_7O_{28}\}$ moieties linked by a single Fe^{III} ion through four Fe–μ_2-O and two P–O bonds, which leads to a previously unobserved sandwich-type structure (Figure 1, a,b) with central symmetry. The basic structural characteristic of $\{HPW_7O_{28}\}$ is similar to the previously reported clusters.[12a,12b] As shown in Figures 1 (a) and 2 (a), this fragment contains one edge-shared W_3O_{13} triad (W1, W2, W3) to which a half-ring of four edge-shaped WO_6 octahedra (W4, W5, W6, W7) is connected through the corners, and this assembly is stabilized by the central PO_4 tetrahedron; the P1–O distances range from 1.517(7) to 1.570(6) Å. Consequently, three tungsten centers of the W_3O_{13} triad have one terminal oxygen atom, whereas the remaining four WO_6 octahedra have two, *cis*-related terminal oxygen groups. Polyanion **1a** does not violate the Lipscomb principle restriction,[3a] which has been explained in terms of the strong *trans* influence of the terminal metal–oxygen bonds that facilitate dissociation of the cluster, and thus, polyoxoanion structures containing three or more terminal oxo groups are not observed.

In $\{HPW_7O_{28}\}$, all tungsten centers are coordinated in a distorted octahedral geometry, and there are four kinds of W–O bonds: the shortest terminal bonds [(W–O_t): 1.694(14)–1.778(14) Å], the double-bridging oxygen bonds

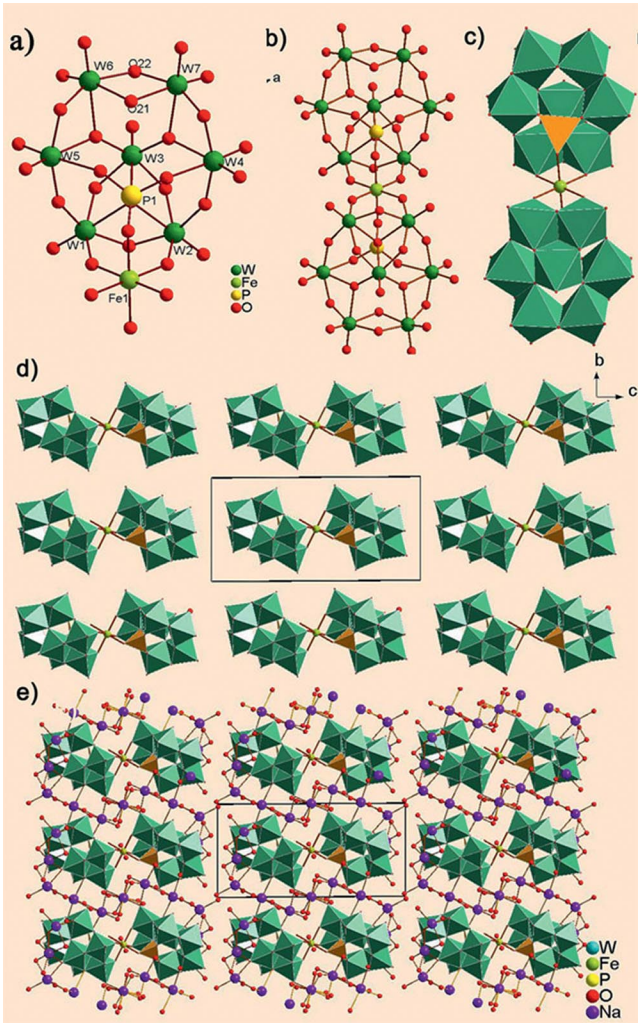

Figure 1. (a) Ball-and-stick representation of the structural subunit of $[PW_7O_{28}]$. (b) Ball-and-stick representation of the structural unit of polyoxoanion of **1**. (c) Polyhedron structure of the polyoxoanion of **1**. The (d) polyoxoanion and (e) molecular packing arrangement of **1** viewed along the *a* axis; gray and orange polyhedra represent WO_6 octahedra and PO_4 tetrahedra, respectively. Hydrogen atoms and lattice water molecules are omitted for clarity.

[(W–μ_2-O_b): 1.758(13)–2.249(6) Å], the triple-bridging oxygen bonds [(W–μ_3-O_b): 1.905(6)–2.283(7) Å], and the longest bonds of the central bridging oxygen atoms [(W–O_c): 2.322(6)–2.461(12) Å]. The central Fe^{III} ion adopts a six-coordinate octahedral geometry with four μ_2-O_b from four WO_6 octahedra of two W_3O_{13} triads [Fe–$O_{12,13}$: 1.984(6)–1.995(6) Å] and another two μ_2-O_b from two central PO_4 tetrahedron groups [Fe–O_{23}:2.039(7) Å]. Selected bond lengths of **1**–**4** are listed in Table 1.

Notably, **1a** is structurally related to the $\{HPW_7O_{28}\}$ and $\{HVW_7O_{28}\}$ units firstly reported in the $[HPW_7O_{28}Ru(dmso)_3]^{6-}$ (**A**)[12a] and $[HVW_7O_{28}Ru(dmso)_3]^{6-}$ (**B**)[12c] polyanions, respectively. The most striking difference among them is that **A** and **B** are open assemblies, in which the $Ru(dmso)_3$ unit is coordinated to $\{HXW_7O_{28}\}$ (X = P for **A**, X = V for **B**) unit through two Ru–O–W bonds and one Ru–O–X bond, respectively. In contrast, **1a** displays a new sandwich-type POM. Moreover, the $\{HPW_7O_{28}\}$ (Figure 2, a) moiety can be viewed as another configuration of the pentalacunary Keggin fragment, which is different from the $\{TeW_7O_{28}\}$ (**C**, Figure 2, b) and $[AsMo_7O_{27}]$ (**D**, Figure 2, c) fragments evident in the $[Te_2W_{16}O_{58}(OH)_2]^{14-}$, $[Te_2W_{18}O_{62}(OH)_2]$,[10–12d] and $[MM'(As^{III}\text{-}Mo_7O_{27})_2]^{12/14-}$ (MM′ = CuCu, CrCr, FeCr, FeFe)[11b] polyoxoanions, respectively. Fragment **C** is thought to originate from the trivacant Keggin-type $\{TeW_9\}$ unit by omitting one edge-shared $\{W_2O_{10}\}$ unit in the equator, which leaves two edge-shared $\{W_2O_{10}\}$ units corner shared. Fragment **D** is usually considered as a monocapped hexavacant α-B-Keggin unit with a central AsO_3 group and can be derived from the trivacant Keggin $[B\text{-}\alpha\text{-}AsMo_9O_{33}]^{9-}$ ion by moving one Mo_3O_{13} triad and inserting one MoO_6 octahedron into the cavity between the two Mo_3O_{13} units.

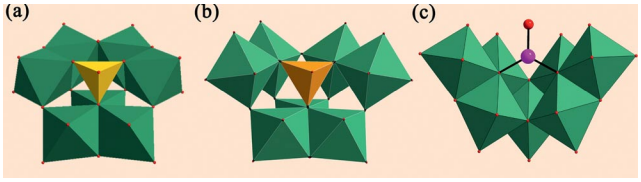

Figure 2. Polyhedron structure of the (a) $\{HPW_7O_{28}\}$, (b) $\{TeW_7O_{28}\}$, and (c) $[AsMo_7O_{27}]$ units. Gold, orange, and purple represent PO_4, TeO_4, and AsO_3, respectively.

It is also of interest to compare **1**–**4** to the manganese-containing pentalacunary HTP $K_{12}Na_1[(HPW_7O_{28})_2\,Mn^{III}]\cdot 17.5H_2O$ (**5**) of Wang and co-workers.[12b] Although they have similar sandwich-type polyanions, the following differences are observed. First, **5** consists of pentalacunary $\{HPW_7O_{28}\}$ units and a Mn^{III} ion, whereas **1**–**4** are made up of $\{HPW_7O_{28}\}$ units and Fe^{III}, Co^{II}, Cd^{II}, and Mn^{II} ions, respectively. Also, **5** was synthesized from the trivacant $Na_8[HPW_9O_{34}]\cdot 24H_2O$ precursor and the manganese $[Mn_{12}(CH_3COO)_{16}(H_2O)_4O_{12}]\cdot 2CH_3COOH\cdot 4H_2O$ cluster rather than simple components, which may be the reason why Wang et al. only obtained manganese-containing HTP. By contrast, we have successfully used an alternative synthetic procedure for the Fe^{III}, Co^{II}, Cd^{II}, and Mn^{II} ana-

Table 1. Selected bond lengths [Å] for **1**–**4**.

A–X	1	2	3	4
W–O_t	1.703(7)–1.751(7)	1.717(6)–1.762(6)	1.715(13)–1.778(14)	1.694(12)–1.728(14)
W–μ_2-O_b	1.813(7)–2.249(6)	1.762(6)–2.249(6)	1.757(13)–2.213(12)	1.758(13)–2.186(12)
W–μ_3-O_b	1.905(6)–2.283(7)	1.926(5)–2.279(6)	1.936(12)–2.253(12)	1.916(11)–2.275(13)
W–O_c	2.343(6)–2.359(6)	2.322(6)–2.413(6)	2.337(11)–2.461(12)	2.339(11)–2.422(11)
P–O	1.517(7)–1.570(6)	1.504(6)–1.595(6)	1.494(14)–1.578(12)	1.529(12)–1.581(11)
X–O	1.984(6)–2.039(7)	2.076(6)–2.140(6)	2.229(13)–2.282(13)	2.145(14)–2.198(12)

logues, which involves the reaction of $Na_2WO_4{\cdot}2H_2O$, H_3PO_4, and CH_3COOH with $FeCl_3{\cdot}6H_2O$, $Co(CH_3COO)_2{\cdot}4H_2O$, $CdSO_4{\cdot}8H_2O$, and $Mn(CH_3COO)_2{\cdot}4H_2O$, respectively, under boiling conditions; this procedure allows the isolation of the sodium salts. If **5** represents the first example of such a HTP, so it is true that **1**–**4** and **5** comprise a new family of sandwich-type POMs constructed from pentalacunary $\{HPW_7O_{28}\}$ units.

The packing arrangement of **1** shows that all the polyanions are parallel to each other (Figure 1, d) and that they are further linked by charge-balanced Na^+ cations to form a 2D structure along the *ab* plane (Figure 1, e). However, in **2**, **3**, and **4**, parallel polyoxoanions connected by Na^+ cations result in 3D supermolecular structures (Figure S3, Supporting Information).

Bond valence sum (BVS) calculations[15] indicate that the oxidation state of all W ions in **1**–**4** are +6 and that the Fe, Co, Cd, and Mn ions in **1**–**4** exhibit an oxidation state of +3, +2, +2, and +2, respectively. Furthermore, the BVS calculations of all the oxygen atoms in the POM fragments were carried out (Table S1, Supporting Information). The values of μ_2-O_{21} in **1** and **3** and those of μ_2-O_{17} in **2** and **4** are in the range of 1.0–1.1, which indicates that these oxygen atoms are monoprotonated. In addition, considering the charge balance of **1**–**4**, some protons need to be added.

IR Spectra

The IR spectra of **1**–**4** (Figures S1 and S2, Supporting Information) are similar in the 600–1000 cm^{-1} region, which is indicative of the W=O and W–O–M vibrations of the POMs. Four characteristic vibration bands assigned to $\nu(W–O_t)$, $\nu(W–\mu_2\text{-}O_b)$, $\nu(W–\mu_3\text{-}O_b)$, and $\nu(W–O_c)$ appear at 941, 916, 889, and 854 cm^{-1} for **1**; 932, 897, 866, and 802 cm^{-1} for **2**; 931, 895, 865, and 802 cm^{-1} for **3**; and 932, 912, 877, and 801 cm^{-1} for **4**, respectively. The stretching resonance in the 1007–1104 cm^{-1} region is ascribed to ν(P–O). However, the vibrational mode of the central PO_4 unit in **1**–**4** is split, and this indicates a structural distortion of the PO_4 tetrahedron.[9o] In addition, the bands at 1635–1648 and 3424–3450 cm^{-1} are attributed to lattice water and ligand water molecules. As above mentioned, the results obtained by IR spectroscopy are well identical with those obtained by X-ray diffraction structural analysis.

UV Spectra

The UV/Vis spectra of **1**–**4** were recorded in aqueous solution (Figure S4, Supporting Information) and in the solid state (Figure S5, Supporting Information). Only one absorption band at approximately 253 nm is observed in the 190–400 nm region, and it is assigned to pπ–dπ charge-transfer transitions of the $O_{b,c}\rightarrow W$ bonds.[16] The bands observed in the spectra of Figure S4 in the near-UV region are possibly due to charge-transfer transitions of the O→M bonds; however, we do not know why it is absent in the case of **3**.

To investigate the influence of pH on the stability of the compounds in aqueous solution, in situ UV/Vis spectroscopic measurements of **1**–**4** were conducted in aqueous

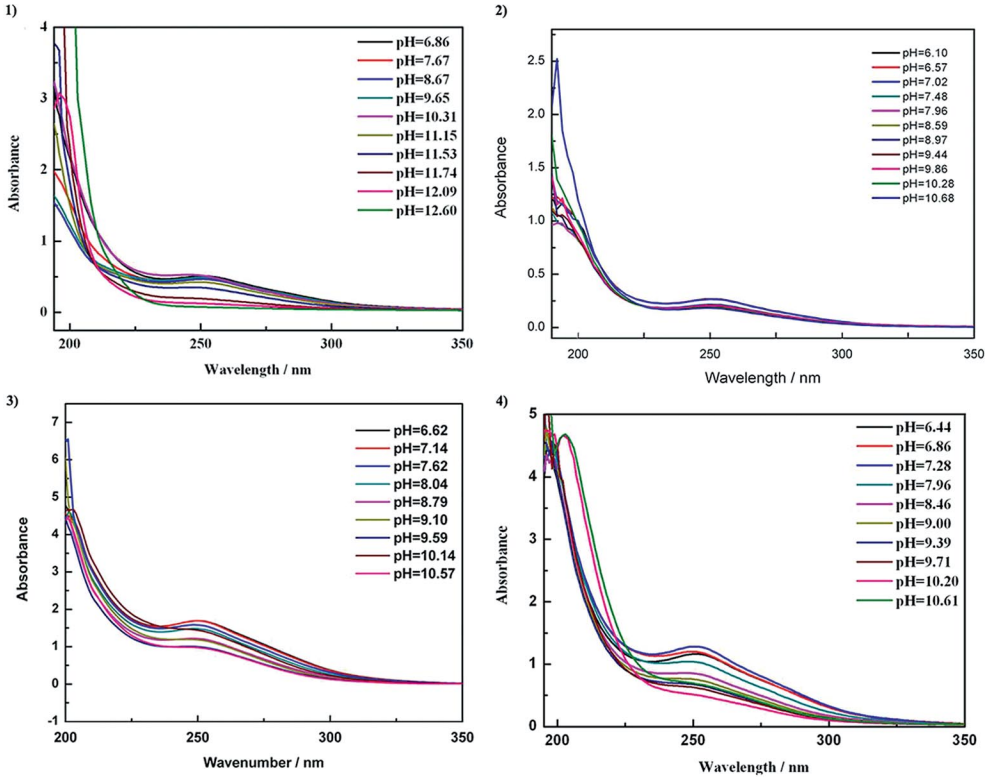

Figure 3. Influence of pH on the stability of **1**–**4** in aqueous solution (2×10^{-4} M).

solution (2×10^{-4} M). The initial pH values of **1**–**4** were 6.86, 6.10, 6.62, and 6.44, respectively. The pH values in the alkaline direction were adjusted by using a dilute NaOH solution. As shown in Figure 3, when the pH value was increased, the absorption band at 253 nm became weaker until it vanished, whereas the absorbance of the solution became stronger, which is a sign for the decomposition of the $[M(HPW_7O_{28})_2]^{n-}$ skeleton of the polyoxoanions. From the aforementioned results, we think that aqueous solutions of **1**–**4** remain stable until the pH value is increased to 10.3, 10.2, 10.1, and 9.7 respectively. In addition, the results of the in situ UV/Vis study of **1** and **3** indicate that they remain stable for at least 6.5 h in aqueous solution at room temperature (Figure S6, Supporting Information).

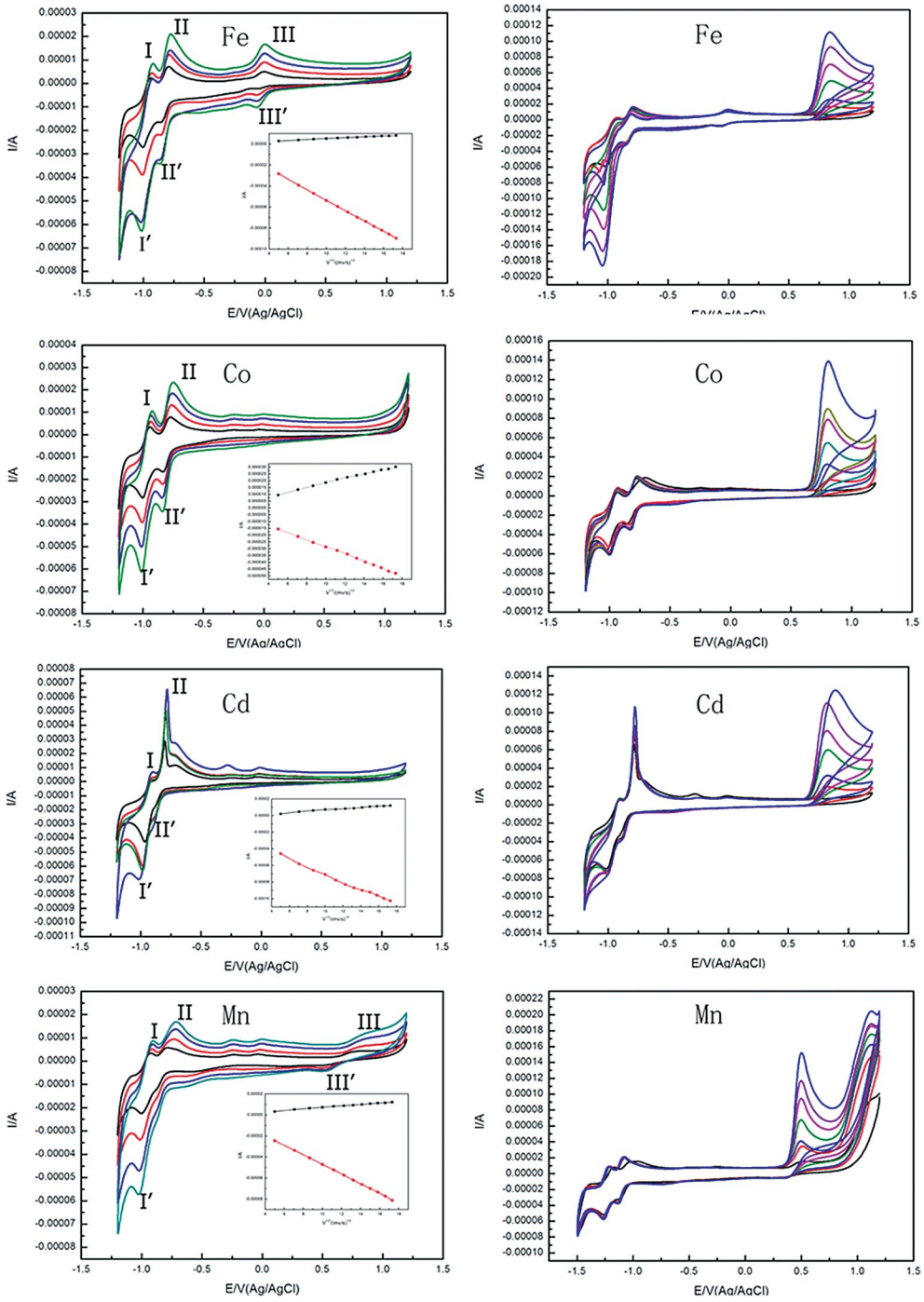

Figure 4. Left: The cyclic voltammograms of 0.1 mM solutions of **1**–**4** in 0.5 M sodium acetate buffer (pH 6.0) at different scan rates (from inner to outer: 25, 50, 100, 150 mV s^{-1}); the inset shows plots of the peak currents (I–I′) against the square root of the scan rates (25, 50, 75, 100, 125, 150, 175, 200, 225, 250, 275, 300 mV s^{-1}). Right: The cyclic voltammograms of 0.1 mM solution of **1**–**4** in 0.5 M sodium acetate buffer (pH 6.0) solution containing 0.0–5.0 mM $NaNO_2$; scan rate: 100 mV s^{-1}. The working electrode was a glassy carbon electrode and the reference electrode was the SCE.

Electrochemistry

The redox properties of **1**–**4** were studied at pH 6.0 in 0.5 M sodium acetate buffer. As shown in Figure 4, two pairs of redox peaks (I–I′, II–II′) are observed, which are attributed to the two consecutive redox processes of W. Relative to the reduction of W^{VI} in **1**, the W^{VI} reductions in **2** and **4** take place at slightly more negative potentials, which is consistent with the more negative charge of the entire polyanion (Figure S7, Supporting Information). In contrast, with an increase in the scan rate, the peak potentials change gradually: the cathodic peak potentials shift towards the negative direction and the corresponding anodic peak potentials shift towards the positive direction. As such, the increasing sizes of the anodic and cathodic peak currents are almost the same, and the peak currents (I–I′) are proportional to the square root of the scan rates (see insets in Figure 4), which indicates that the redox processes are diffusion-confined over a specific range of scan rates.[17] For compounds **1** and **4**, it was possible to detect the third defined oxidation peak centered at +0.007 and +0.504 V, respectively, which can be ascribed to the reduction of the Fe^{III} centers to Fe^{II}[9m] and the oxidation of the Mn^{II} centers to Mn^{III},[18] respectively. However, there is no peak for Co^{II} and Cd^{II} in the cyclic voltammetry (CV) curves of **2** and **3** upon a scan in the negative direction, which is in accordance with the fact that polyanions **2** and **3** cannot be further oxidized or reduced, and hence, only the tungsten redox waves are observed. Furthermore, the CV patterns suggest that **1**–**4** are stable in 0.5 M sodium acetate buffer media (pH 6.0) over at least 7 h (Figure S8, Supporting Information).

The elimination of nitrite ions in environmental and food samples has been drawing considerable attention in recent years as a result of their distinct toxicity and suspected carcinogenicity.[19] Interestingly, POMs are appropriate candidates for catalysts because they have the ability to deliver electrons to other species and thus serve as powerful electron reservoirs for mutielectron reductions.[20] In this context, the exploration of new POM catalysts modified on the electrode is a continuing research topic.

For this reason, the electrocatalytic reduction of nitrite by **1**–**4** was also investigated in the same buffer solution as that employed in the CV studies, and the results demonstrate that only compound **1** exhibits moderately good electrocatalytic activity towards the reduction of nitrite (Figure 4, right, top). With stepwise addition of modest amounts of nitrite, the I′ and II′ reduction peak currents of W increased, whereas the corresponding oxidation peak currents significantly decreased, and this implies that nitrite was reduced by the reduced POM species. Obviously, there is an irreversible oxidation that appears in the cyclic voltammograms as the nitrite is added, and this is expected for NO_2^-. This assumption is corroborated by the cyclic voltammograms of 0.5 M sodium acetate buffer (pH 6.0) solution containing 0.0–5.0 mM $NaNO_2$ in the absence of **1** (Figure S9, Supporting Information).

Thermogravimetric Analysis

To examine the thermal stabilities of **1**–**4**, thermogravimetric (TG) analyses were carried out under a N_2 atmosphere. The TG curves all show a continuous one-step weight loss (Figure S10, Supporting Information) from 55 to about 380 °C, which can be ascribed to the loss of lattice and protonated water molecules. The observed weight loss of 16.40% is consistent with the calculated value of 17.60%, which corresponds to the endothermic peak at 57 °C in the differential scanning calorimetry (DSC) curve of **1** (Figure 5), whereas the very strong exothermal peak at 474 °C may be attributed to the collapse or the structural change of the POM framework. The TG curves of **2**, **3**, and **4** are very similar to that of **1**, and the total weight loss is 16.65% (calcd. 17.23%) for **2**, 16.17% (calcd. 17.03%) for **3**, and 16.38% (calcd. 17.24%) for **4**. In addition, there is no further weight loss until 600 °C.

Conclusions

In summary, four new HPTs $Na_{12}H[Fe(HPW_7O_{28})_2]\cdot 44H_2O$ (**1**), $Na_{14}[M(HPW_7O_{28})_2]\cdot 44H_2O$ {M = Co^{II} (**2**), Cd^{II} (**3**), Mn^{II} (**4**)} were prepared by conventional beaker methods. Compounds **1**–**4** along with $K_{12}Na_1[(HPW_7O_{28})_2\text{-}Mn^{III}]\cdot 17.5H_2O$ reported before represent a new family of

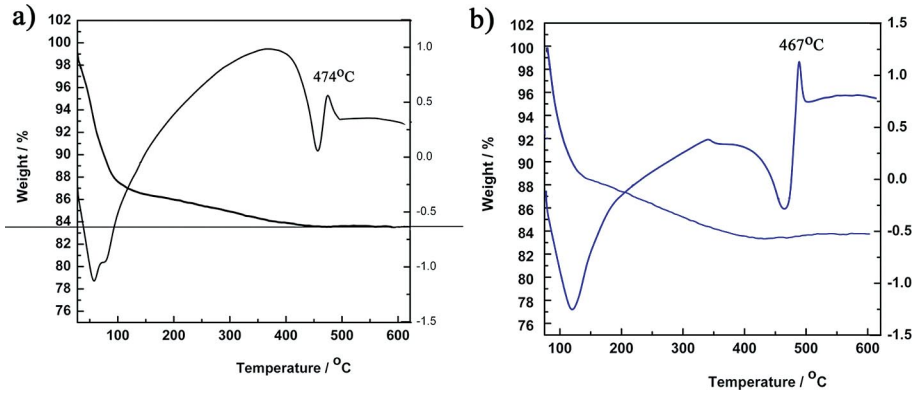

Figure 5. TG-DSC curves of (a) **1** and (b) **3**.

sandwich-type POMs, in which a single Fe^{III}, Co^{II}, Cd^{II}, Mn^{II}, and Mn^{III} ion is sandwiched between two rare $\{HPW_7O_{28}\}$ subunits. The compounds reported here enrich the structural diversity of TM-substituted HPTs, and they may be used in feasible and effective synthetic routes in the search and exploration of other high-lacunary POM-based sandwich-type frameworks having potential applications in organocatalysis. Furthermore, compound **1** seems to be effective at catalyzing the reduction of nitrite. Efforts to prepare POMs constructed from higher lacunary Keggin and Dawson building blocks or larger metal cluster aggregates with high-dimensional structures are in progress.

Experimental Section

Materials and Methods: All reagents were used as purchased without further purification. IR spectra were recorded with a Nicolet FTIR 360 spectrometer by using KBr pellets in the range of 4000–400 cm^{-1}. UV absorption spectra were obtained with a U-4100 spectrometer (distilled water as solvent) at 190–400 nm at room temperature. TG analyses were carried out under N_2 flow with a Mettler-Toledo TGA/SDTA 851^e instrument at a heating rate of 10 °C min^{-1} up to 600 °C. All electrochemical measurements were performed at room temperature in a standard three-electrode cell connected to a LK98 microcomputer-based electrochemical system (LANLIKE, Tianjin, China). A freshly cleaned glassy carbon disk electrode (3 mm diameter) was used as the working electrode, a platinum wire served as the counterelectrode, and an Ag/AgCl electrode was used as the reference electrode.

Synthesis of 1: A sample of $Na_2WO_4{\cdot}2H_2O$ (5.000 g, 15.158 mmol) was dissolved in distilled water (10 mL). Then, 85% H_3PO_4 (0.17 mL, 2.93 mmol) and CH_3COOH (0.60 mL, 10.64 mmol) were added successively. The mixture was heated to boiling with vigorous stirring, followed by the addition of a solution of $FeCl_3{\cdot}6H_2O$ (0.296 g, 1.095 mmol) in distilled water (3 mL). This solution was heated at reflux for 30 min and then cooled to room temperature and filtered. The final pH value was 8.0. After approximately 4 h, a large amount of greenish yellow block crystals were obtained, yield 50.2% (based on $Na_2WO_4{\cdot}2H_2O$). $H_{91}FeNa_{12}O_{100}P_2W_{14}$ (4659.23): calcd. H 1.97, Na 5.92, P 1.33, Fe 1.20, W 55.24; found H 1.93, Na 6.84, P 1.32, Fe 1.17, W 54.72. IR (KBr): $\tilde{\nu}$ = 3424 (s), 1647 (m), 1068 (s), 1010 (w), 941 (s), 916 (s), 889 (s), 804 (s), 674 (s), 525 (s) cm^{-1}.

Synthesis of 2: A sample of $Na_2WO_4{\cdot}2H_2O$ (5.000 g, 15.158 mmol) was dissolved in distilled water (10 mL). Then, 85% H_3PO_4 (0.17 mL, 2.93 mmol) and CH_3COOH (0.50 mL, 8.87 mmol) were added successively. The mixture was heated to boiling with vigorous stirring, followed by the addition of a solution of $Co(CH_3COO)_2{\cdot}4H_2O$ (0.130 g, 0.522 mmol) in distilled water (3 mL). This solution was heated at reflux for 20 min and then cooled to room temperature and filtered. The final pH value was 8.3. After 8 d, pink block crystals were collected, yield 12.1% [based on $Co(CH_3COO)_2{\cdot}4H_2O$]. $H_{90}CoNa_{14}O_{100}P_2W_{14}$ (4707.29): calcd. H 1.93, Na 6.84, P 1.32, Co 1.25, W 54.68; found H 1.88, Na 7.12, P 1.35, Co 1.34, W 55.17. IR (KBr): $\tilde{\nu}$ = 3425 (s), 1635 (m), 1088 (s), 1007 (w), 932 (s), 897 (s), 866 (s), 802 (s), 693 (s), 527 (s) cm^{-1}.

Synthesis of 3: The preparation of **3** was similar to that of **2** except that $CdSO_4{\cdot}8H_2O$ (0.275 g, 0.357 mmol) was used instead of $Co(CH_3COO)_2{\cdot}4H_2O$. The final pH value was 8.6. A large amount of colorless block crystals were isolated on the next day, yield 38.8% (based on $Na_2WO_4{\cdot}2H_2O$). $H_{90}CdNa_{14}O_{100}P_2W_{14}$ (4760.76): calcd. H 1.90, Na 6.76, P 1.30, Cd 2.36, W 54.06; found H 1.87, Na 6.92, P 1.34, Cd 2.19, W 55.18. IR (KBr): $\tilde{\nu}$ = 3437 (s), 1634 (m), 1104 (s), 1064 (s), 1007(w), 931 (s), 895 (s), 865 (s), 802 (s), 698 (s), 517 (s) cm^{-1}.

Synthesis of 4: The preparation of **4** was similar to that of **2** except that $Mn(CH_3COO)_2{\cdot}4H_2O$ (0.362 g, 1.477 mmol) was used instead of $Co(CH_3COO)_2{\cdot}4H_2O$. The final pH value was 8.0. After 5 d, yellow flake-like crystals were collected, yield 16.1% (based on $Na_2WO_4{\cdot}2H_2O$). $H_{90}MnNa_{14}O_{100}P_2W_{14}$ (4703.29): calcd. H 1.93, Na 6.84, P 1.32, Mn 1.17, W 54.72; found H 1.98, Na 7.04, P 1.38, Mn 1.28, W 53.82. IR (KBr): $\tilde{\nu}$ = 3447 (s), 1636 (m), 1091 (s), 1068 (s), 1007(w), 932 (s), 912 (s), 877 (s), 801 (s), 688 (s), 525 (s) cm^{-1}.

Table 2. Crystallographic data and structural refinements for **1**–**4**.

	1	**2**	**3**	**4**
Formula	$Na_{12}H_{91}P_2W_{14}FeO_{100}$	$Na_{14}H_{90}P_2W_{14}CoO_{100}$	$Na_{14}H_{90}P_2W_{14}CdO_{100}$	$Na_{14}H_{90}P_2W_{14}MnO_{100}$
M_r / g mol^{-1}	4659.09	4707.15	4760.63	4703.16
T / K	296(2)	296(2)	296(2)	296(2)
Space group	$P\bar{1}$	$P\bar{1}$	$P\bar{1}$	$P\bar{1}$
Crystal system	triclinic	triclinic	triclinic	triclinic
a / Å	10.5424(5)	11.910(2)	11.8560(12)	11.844(8)
b / Å	10.9863(5)	12.150(2)	12.1098(13)	12.084(8)
c / Å	20.9810(11)	17.916(3)	18.085(2)	17.971(12)
α / °	84.9890(10)	79.879(3)	80.339(2)	79.906(13)
β / °	77.7830(10)	85.227(3)	85.509(3)	85.459(13)
γ / °	67.4310(10)	60.813(3)	60.826(2)	60.924(10)
V / Å^3	2193.09(18)	2228.0(7)	2235.0(4)	2213(3)
Z	1	1	1	1
D_c / g cm^{-3}	3.526	3.507	3.536	3.528
μ / mm^{-1}	18.668	18.409	18.404	18.489
Limiting indices	$-12 \le h \le 12$	$-13 \le h \le 14$	$-14 \le h \le 12$	$-14 \le h \le 10$
	$-13 \le k \le 9$	$-9 \le k \le 14$	$-14 \le k \le 14$	$-14 \le k \le 14$
	$-22 \le l \le 24$	$-20 \le l \le 21$	$-19 \le l \le 21$	$-21 \le l \le 21$
GOF on F^2	1.042	1.026	1.037	1.009
R_1[a], wR_2[b] [$I > 2\sigma(I)$]	0.0379, 0.1024	0.0333, 0.0836	0.0436, 0.1072	0.0571, 0.1059
R_1[a], wR_2[b] (all data)	0.0434, 0.1051	0.0380, 0.0854	0.0498, 0.1097	0.0980, 0.1162

[a] $R_1 = \Sigma||F_o| - |F_c||/\Sigma|F_o|$. [b] $wR_2 = [\Sigma w(F_o^2 - F_c^2)^2/\Sigma w(F_o^2)^2]^{1/2}$.

Crystallographic Data Collection and Refinement: Intensity data for compounds **1**–**4** were collected with a Bruker Apex-II CCD diffractometer with Mo-K_α-monochromated radiation (λ = 0.71073 Å) at 296(2) K. The structures were solved by direct methods and refined by full-matrix least-squares methods on F^2 with the SHELXTL-97 program package.[21] Intensity data were corrected for Lorentz and polarization effects as well as for multiscan absorption. No hydrogen atoms associated with the molecules were located from the difference Fourier map. All of the non-hydrogen atoms were refined anisotropically except for some water molecules. A summary of the crystallographic data and structural refinements for **1**–**4** are summarized in Table 2.

Further details on the crystal structure investigations may be obtained from the Fachinformationszentrum Karlsruhe, 76344 Eggenstein-Leopoldshafen, Germany (fax: +49-7247-808-666; e-mail: crysdata@fiz-karlsruhe.de), on quoting the depository number CSD-424023 (for **1**), -424024 (for **2**), -424025 (for **3**), and -424026 (for **4**).

Supporting Information (see footnote on the first page of this article): Additional molecular packing arrangement of **2**; cyclic voltammograms, TG curves, and IR spectra of **1**–**4**; UV/Vis spectra of **1**–**4** in aqueous solution; solid state UV/Vis spectra of **1**–**4**; in situ UV/Vis spectra of **1** and **3**; the aging cyclic voltammograms. of **1**–**4**; BVS values of all the oxygen atoms except the lattice water molecules in **1**–**4**.

Acknowledgments

We gratefully acknowledge financial support from the Natural Science Foundation of China (NSFC) (grant numbers 21071042, 21171048, and 21172052), Natural Science Foundation of Henan Province (grant numbers 092102210151, 102102210023, and 122300410126), Excellent Scientist Fund in Henan Province (grant number 094200510001), and the Scientific and Technological Innovation Team of Henan Province (grant number 2010IRTSTHN011).

[1] a) P. Gouzerh, A. Proust, *Chem. Rev.* **1998**, *98*, 77–111; b) D. L. Long, R. Tsunashima, L. Cronin, *Angew. Chem.* **2010**, *122*, 1780–1803; *Angew. Chem. Int. Ed.* **2010**, *49*, 1736–1758.

[2] a) S. T. Zheng, J. Zhang, X. X. Li, W. H. Fang, G. Y. Yang, *J. Am. Chem. Soc.* **2010**, *132*, 15102–15103; b) A. Dolbecq, E. Dumas, C. R. Mayer, P. Mialane, *Chem. Rev.* **2010**, *110*, 6009–6048; c) J. Y. Niu, P. T. Ma, H. Y. Niu, J. Li, J. W. Zhao, Y. Song, J. P. Wang, *Chem. Eur. J.* **2007**, *13*, 8739–8748; d) F. Y. Li, L. Xu, *Dalton Trans.* **2011**, *40*, 4024–4034.

[3] a) M. T. Pope, *Heteropoly and Isopoly Oxometalates*, Springer, Berlin, **1983**; b) T. Yamase, *Chem. Rev.* **1998**, *98*, 307–326.

[4] a) D. L. Long, E. Burkholder, L. Cronin, *Chem. Soc. Rev.* **2007**, *36*, 105–121; b) D. E. Katsoulis, *Chem. Rev.* **1998**, *98*, 359–387; c) J. T. Rhule, W. A. Neiwert, K. I. Hardcastle, B. T. Do, C. L. Hill, *J. Am. Chem. Soc.* **2001**, *123*, 12101–12102; d) U. Kortz, A. Müller, J. van Slageren, J. Schnack, N. S. Dalal, M. Dressel, *Coord. Chem. Rev.* **2009**, *253*, 2315–2327; e) H. E. Moll, W. Zhu, E. Oldfield, L. M. Rodriguez-Albelo, P. Mialane, J. Marrot, N. Vila, I. M. Mbomekallé, E. Rivière, C. Duboc, A. Dolbecq, *Inorg. Chem.* **2012**, *51*, 7921–7931; f) M. Nyman, *Dalton Trans.* **2011**, *40*, 8049–8058.

[5] a) A. P. Ginsbergh (Ed.), *Inorganic Syntheses*, Wiley, **1990**, vol. 27, pp. 85–111; b) N. Haraguchi, Y. Okaue, T. Isobe, Y. Matsuda, *Inorg. Chem.* **1994**, *33*, 1015–1020; c) R. Contant, A. Tézé, *Inorg. Chem.* **1985**, *24*, 4610–4614.

[6] a) C. L. Hill, X. Zhang, *Nature* **1995**, *373*, 324–326; b) S. W. Zhang, J. W. Zhao, P. T. Ma, J. Y. Niu, J. P. Wang, *Chem. Asian J.* **2012**, *7*, 966–974; c) J. Y. Niu, X. Q. Zhang, D. H. Yang, J. W. Zhao, P. T. Ma, U. Kortz, J. P. Wang, *Chem. Eur. J.* **2012**, *18*, 6759–6762; d) Y. Xu, X. H. Bu, N. K. Goh, L. S. Chia, G. D. Stucky, *J. Chem. Soc., Dalton Trans.* **2001**, 2009–2014; e) C. M. Wang, S. T. Zheng, G. Y. Yang, *Inorg. Chem.* **2007**, *46*, 616–618; f) H. Y. An, Z. B. Han, T. Q. Xu, *Inorg. Chem.* **2010**, *49*, 11403–11414; g) L. Lisnard, P. Mialane, A. Dolbecq, J. Marrot, J. M. Clemente-Juan, E. Coronado, B. Keita, P. de Oliveira, L. Nadjo, F. Sécheresse, *Chem. Eur. J.* **2007**, *13*, 3525–3536.

[7] a) H. Weiner, H. J. Lunk, R. Friese, H. Hartl, *Inorg. Chem.* **2005**, *44*, 7751–7761; b) M. Sadakane, D. Tsukuma, M. H. Dickman, B. S. Bassil, U. Kortz, M. Capron, W. Ueda, *Dalton Trans.* **2007**, 2833–2838; c) C. Pichon, A. Dollbecq, P. Mialane, J. Marrot, E. Rivière, M. Goral, M. Zynek, T. McCormac, S. A. Borshch, E. Zueva, F. Sécheresse, *Chem. Eur. J.* **2008**, *14*, 3189–3189; d) A. Sartorel, G. Scorrano, H. Oelrich. L. Walder, M. Bonchio, U. Kortz, *Inorg. Chem.* **2010**, *49*, 7–9.

[8] a) U. Kortz, Y. P. Jeannin, A. Tézé, G. Hervé, S. Isber, *Inorg. Chem.* **1999**, *38*, 3670–3675; b) B. Botar, P. Kögerler, C. L. Hill, *Inorg. Chem.* **2007**, *46*, 5398–5403; c) S. Yamaguchi, Y. Kikukawa, K. Tsuchida, Y. Nakagawa, K. Uehara, K. Yamaguchi, N. Mizuno, *Inorg. Chem.* **2007**, *46*, 8502–8504; d) A. Yoshida, Y. Nakagawa, K. Uehara, S. Hikichi, N. Mizuno, *Angew. Chem.* **2009**, *121*, 7189–7192; *Angew. Chem. Int. Ed.* **2009**, *48*, 7055–7058; e) B. S. Bassil, M. Ibrahim, R. Al-Oweini, M. Asano, Z. X. Wang, J. V. Tol, N. S. Dalal, K. Y. Choi, R. N. Biboum, B. Keita, L. Nadjo, U. Kortz, *Angew. Chem.* **2011**, *123*, 6083–6087; *Angew. Chem. Int. Ed.* **2011**, *50*, 5961–5964.

[9] a) M. Bösing, A. Nöh, I. Loose, B. Krebs, *J. Am. Chem. Soc.* **1998**, *120*, 7252–7259; b) U. Kortz, N. K. Al-Kassem, M. G. Savelieff, N. A. Al Kadi, M. Sadakane, *Inorg. Chem.* **2001**, *40*, 4742–4749; c) H. Andres, J. M. Clemente-Juan, R. Basler, H. U. Güdel, J. J. Borrás-Almenar, A. Gaita, E. Coronado, H. Büttner, S. Janssen, *Inorg. Chem.* **2001**, *40*, 1943–1950; d) J. M. Clemente-Juan, E. Coronado, A. Gaita-Ariño, C. Giménez-Saiz, G. Chaboussant, H. U. Güdel, R. Burriel, H. Mutka, *Chem. Eur. J.* **2002**, *8*, 5701–5708; e) M. D. Ritorto, T. M. Anderson, W. A. Neiwert, C. L. Hill, *Inorg. Chem.* **2004**, *43*, 44–49; f) S. Nellutla, J. van Tol, N. S. Dalal, L. H. Bi, U. Kortz, B. Keita, L. Nadjo, G. A. Khitrov, A. G. Marshall, *Inorg. Chem.* **2005**, *44*, 9795–9806; g) J. Wang, P. Ma, Y. Shen, J. Niu, *Cryst. Growth Des.* **2007**, *7*, 603–605; h) Z. M. Zhang, Y. F. Qi, C. Qin, Y. G. Li, E. B. Wang, X. L. Wang, Z. M. Su, L. Xu, *Inorg. Chem.* **2007**, *46*, 8162–8169; i) S. T. Zheng, D. Q. Yuan, H. P. Jia, J. Zhang, G. Y. Yang, *Chem. Commun.* **2007**, 1858–1860; j) J. W. Zhao, H. P. Jia, J. Zhang, S. T. Zheng, G. Y. Yang, *Chem. Eur. J.* **2007**, *13*, 10030–10045; k) J. P. Wang, P. T. Ma, J. Li, H. Y. Niu, J. Y. Niu, *Chem. Asian J.* **2008**, *3*, 822–833; l) S. T. Zheng, J. Zhang, J. M. Clemente-Juan, D. Q. Yuan, G. Y. Yang, *Angew. Chem.* **2009**, *121*, 7312–7315; *Angew. Chem. Int. Ed.* **2009**, *48*, 7176–7179; m) J. D. Compain, P. Mialane, A. Dolbecq, I. M. Mbomekallé, J. Marrot, F. Sécheresse, E. Rivière, G. Rogez, W. Wernsdorfer, *Angew. Chem.* **2009**, *121*, 3123–3127; *Angew. Chem. Int. Ed.* **2009**, *48*, 3077–3081; n) Y. Kikukawa, K. Yamaguchi, N. Mizuno, *Inorg. Chem.* **2010**, *49*, 8194–8196; o) Y. Hou, L. Xu, M. J. Cichon, S. Lense, K. I. Hardcastle, C. L. Hill, *Inorg. Chem.* **2010**, *49*, 4125–4132; p) I. V. Kalinina, N. V. Izarova, U. Kortz, *Inorg. Chem.* **2012**, *51*, 7442–7444; q) D. D. Zhang, C. Z. Wang, S. Z. Li, J. P. Liu, P. T. Ma, J. P. Wang, J. Y. Niu, *J. Solid State Chem.* **2013**, *198*, 18–23.

[10] a) P. Mialane, A. Dolbecq, J. Marrot, E. Rivière, F. Sécheresse, *Chem. Eur. J.* **2005**, *11*, 1771–1778; b) B. S. Bassil, S. Nellutla, U. Kortz, A. C. Stowe, J. van Tol, N. S. Dalal, B. Keita, L. Nadjo, *Inorg. Chem.* **2005**, *44*, 2659–2665; c) N. H. Nsouli, A. H. Ismail, I. S. Helgadottir, M. H. Dickman, J. M. Clemente-Juan, U. Kortz, *Inorg. Chem.* **2009**, *48*, 5884–5890.

[11] a) L. L. Li, Q. Sheng, G. L. Xue, H. S. Xu, H. M. Hu, F. Fu, J. W. Wang, *Dalton Trans.* **2008**, 5698–5700; b) H. S. Xu, L. L. Li, B. Liu, G. L. Xue, H. M. Hu, F. Fu, J. W. Wang, *Inorg. Chem.* **2009**, *48*, 10275–10280; c) B. Liu, L. L. L. Li, Y. P.

Zhang, Y. Ma, H. M. Hu, G. L. Xue, *Inorg. Chem.* **2011**, *50*, 9172–9177; d) X. Q. Dong, Y. P. Zhang, B. Liu, Y. Z. Zhen, H. M. Hu, G. L. Xue, *Inorg. Chem.* **2012**, *51*, 2318–2324.

[12] a) L. H. Bi, M. H. Dikman, U. Kortz, I. Dix, *Chem. Commun.* **2005**, 3962–3964; b) Q. Wu, Y. Y. Li, Y. H. Wang, Z. M. Zhang, E. B. Wang, *Inorg. Chem. Commun.* **2010**, *13*, 66–69; c) L. H. Bi, B. Wang, G. F. Hou, B. Li, L. X. Wu, *CrystEngComm* **2010**, *12*, 3511–3514; d) C. Ritchie, K. G. Alley, C. Boskovic, *Dalton Trans.* **2010**, *39*, 8872–8874.

[13] S. S. Mal, U. Kortz, *Angew. Chem.* **2005**, *117*, 3843–3846; *Angew. Chem. Int. Ed.* **2005**, *44*, 3777–3780.

[14] J. J. Borras-Almenar, J. M. Clemente-Juan, M. Clemente-Juan, E. Coronado, J. R. Galan-Mascaros, C. J. Gómez-García, in: *Polyoxometalate Chemistry: From Topology via Self-Assembly to Applications* (Eds.: M. T. Pope, A. Müller), Dordrecht, The Netherlands, **2001**, p. 231.

[15] I. D. Brown, D. Altermat, *Acta Crystallogr., Sect. B* **1985**, *41*, 244–247.

[16] J. P. Wang, X. Y. Duan, X. D. Du, J. Y. Niu, *Cryst. Growth Des.* **2006**, *6*, 2266–2270.

[17] a) Z. G. Han, Y. L. Zhao, J. Peng, Y. H. Feng, J. N. Yin, Q. Liu, *Electroanalysis* **2002**, *17*, 1097–1102; b) W. L. Yun, Y. G. Li, Y. H. Wang, X. J. Feng, L. Ying, E. B. Wang, *Inorg. Chem.* **2009**, *48*, 6452–6458.

[18] S. G. Mitchell, T. Boyd, H. N. Miras, D. L. Long, L. Cronin, *Inorg. Chem.* **2011**, *50*, 136–143.

[19] a) A. Belhouari, B. Keita, L. Nadjo, R. Contant, *New J. Chem.* **1998**, *22*, 83–87; b) B. S. Bassil, U. Kortz, A. S. Tigan, J. M. Clemente-Juan, B. Keita, D. P. Oliveira, L. Nadjo, *Inorg. Chem.* **2005**, *44*, 9360–9368.

[20] a) T. McCormac, D. Farrell, D. G. Drennan, *Electroanalysis* **2001**, *13*, 836–842; b) S. Cheng, T. Fernandez-Otero, E. Coronado, C. J. Gomez-Garcia, E. Martinez-Ferrero, C. J. Gimenez-Saiz, *Phys. Chem. B* **2002**, *106*, 7585–7591; c) B. Keita, I. M. Mbomekalle, L. Nadjo, *Electrochem. Commun.* **2003**, *5*, 830–837; d) X. L. Wang, Z. H. Kang, E. B. Wang, C. W. Hu, *J. Electroanal. Chem.* **2002**, *523*, 142–149.

[21] a) G. M. Sheldrick, *SHELXS97*, *Program for Crystal Structure Solution*, University of Göttingen, Germany, **1997**; b) G. M. Sheldrick, *SHELXL97, Program for Crystal Structure Refinement*, University of Göttingen, Germany, **1997**.

Received: September 16, 2012
Published Online: December 6, 2012

